Reallocation of elemental content and macromolecule in the coccolithophore _Emiliania huxleyi_ to acclimate to climate change

Yong Zhang[1],*, Yong Zhang[1,§], Shuai Ma[1], Hanbing Chen[2], Jiabing Li[1], Zhengke Li[3], Kui Xu[4], Ruiping Huang[5], Hong Zhang[1], Yonghe Han[1], Jun Sun[6]

[1]College of Environmental and Resource Sciences, College of Carbon Neutral Modern Industry, Fujian Key Laboratory of Pollution Control and Resource Recycling, Fujian Normal University, Fuzhou, China

[2]College of Life Science, Fujian Normal University, Fuzhou, China

[3]School of Food and Biological Engineering, Shanxi University of Science and Technology, Xi'an, China

[4]Hubei Key Laboratory of Edible Wild Plants Conservation and Utilization, Hubei Engineering Research Center of Special Wild Vegetables Breeding and Comprehensive Utilization Technology, College of Life Sciences, Hubei Normal University, Huangshi, China

[5]State Key Laboratory of Marine Environmental Science, College of Ocean and Earth Sciences, Xiamen University, Xiamen, China

[6]Institute for Advanced Marine Research, China University of Geosciences, Guangzhou, China

Running head: Physiology and biochemistry of *E. huxleyi*

*Correspondence: Yong Zhang (yongzhang@fjnu.edu.cn)

Keywords: Carbohydrate; CO_2; coccolithophore; elemental content; light intensity; phosphorus availability; protein.

§Email: qsx20211022@student.fjnu.edu.cn

Abstract

Global climate change leads to simultaneous changes in multiple environmental drivers in the marine realm. Although physiological characterization of coccolithophores have been studied under climate change, there is limited knowledge on the biochemical responses of this biogeochemically important phytoplankton group to changing multiple environmental drivers. Here we investigate the interactive effects of reduced phosphorus availability (4 to 0.4 μmol L^{-1}), elevated pCO$_2$ concentrations (426 to 946 μatm) and increasing light intensity (40 to 300 μmol photons m^{-2} s^{-1}) on elemental content and macromolecules of the cosmopolitan coccolithophore *Emiliania huxleyi*. Reduced phosphorus availability reduces particulate organic nitrogen and protein contents per cell under 40 μmol photons m^{-2} s^{-1}, but not under 300 μmol photons m^{-2} s^{-1}. Reduced phosphorus availability and elevated pCO$_2$ concentrations act synergistically to increase particulate organic carbon (POC) and carbohydrate contents per cell under 300 μmol photons m^{-2} s^{-1} but not under 40 μmol photons m^{-2} s^{-1}. Reduced phosphorus availability, elevated pCO$_2$ concentrations and increasing light intensity act synergistically to increase the allocation of POC to carbohydrates. Under elevated pCO$_2$ concentrations and increasing light intensity, enhanced carbon fixation could increase carbon storage in the phosphorus-limited regions of the oceans where *E. huxleyi* dominates the phytoplankton assemblages. In each light intensity, elemental carbon to phosphorus (C : P) and nitrogen to phosphorus (N : P) ratios decrease with increasing growth rate. These results suggest that coccolithophores could reallocate chemical elements and energy to synthesize macromolecules efficiently, which allows them to regulate its elemental content and growth rate to acclimate to changing environmental conditions.

1 Introduction

Continuous increase in atmospheric CO_2 level, as a consequence of anthropogenic activities, leads to global and ocean warming, which in turn shoals the ocean upper mixed layer (UML), hinders upward transport of nutrients from deeper ocean to the UML and increases light exposures to phytoplankton cells dwelling therein (Steinacher et al., 2010; Wang et al., 2015). The dissolution of CO_2 in the oceans is causing a significant chemical shift toward higher CO_2 and proton ($[H^+]$) concentrations, a process defined as ocean acidification (OA) (Caldeira and Wickett, 2003). Environmental changes in the UML will expose phytoplankton cells to physiological stress, and understanding the effects of changing multiple environmental drivers on the physiology and biochemistry of marine phytoplankton is important for projections of changes in the biogeochemical roles of phytoplankton in the future ocean (Gao et al., 2019).

Coccolithophores take up carbon dioxide (CO_2) to produce particulate organic carbon (POC) via photosynthesis, and use bicarbonate (HCO_3^-) and calcium (Ca^{2+}) to synthesize calcium carbonate plates (coccoliths, PIC) and release CO_2 via calcification, and play a critical role in the marine carbon cycle (Rost and Riebesell, 2004). The cosmopolitan coccolithophore *Emiliania huxleyi* typically forms extensive blooms that are easily detected by satellite remote sensing due to high light scattering caused by coccoliths (Terrats et al., 2020; He et al., 2022). Within *E. huxleyi* blooms in polar and subpolar oceans, dissolved nitrate and phosphate concentrations in surface seawater could be as lower as 0.95 μmol L^{-1} and 0.16 μmol L^{-1}, respectively (Townsend et al., 1994), light intensity are higher than 300 μmol photons m^{-2} s^{-1} (Tyrrell and Merico, 2004), and the mean concentrations of seawater CO_2 increased by 21.0%–43.3% which weakens the oceanic CO_2 uptake from the atmosphere

(Kondrik et al., 2018). *Emiliania huxleyi* is also the dominant phytoplankton species in the lower photic zone in the north-eastern Caribbean Sea (western Atlantic Ocean) (Jordan and Winter, 2000) and in the South Pacific Gyre where dissolved nitrate and phosphate concentration are about 1.0 μmol L^{-1} and 0.2 μmol L^{-1}, respectively, and light intensity is lower than 20 μmol photons m^{-2} s^{-1} (Beaufort et al., 2008; Perrin et al., 2016). In the future ocean, numerous environmental factors will simultaneously change and the extent of these changes may increase (Gao et al., 2019). To explore how *E. huxleyi* acclimate to simultaneous changes in macronutrient concentration, light intensity and CO_2 level, it is interesting to investigate their physiological and biochemical processes, which can also help to project the effect of coccolithophores on ocean carbon cycle and ecological systems.

For more than a decade, research has shown that *E. huxleyi* cells developed several strategies to acclimate to reduced phosphorus availability, increasing light intensity and ocean acidification (Leonardos and Geider, 2005; McKew et al., 2015; Wang et al., 2022). Interactive effects of phosphorus availability and light intensity have shown that under phosphorus limitation condition, cells increased expression and the activity of alkaline phosphatase, and took up and used phosphorus efficiently under high light intensity, whereas they lowered the phosphorus uptake rate under low light intensity (Riegman et al., 2000; Perrin et al., 2016). In addition, the positive effect of reduced phosphorus availability on cellular POC and PIC contents of *E. huxleyi* was further enhanced by increasing light intensity due to high-light-induced increases in CO_2 and HCO_3^- uptake rates under low phosphate availability (Leonardos and Geider, 2005). The negative effect of reduced phosphorus availability on cellular particulate organic phosphorus (POP) content was partly compensated by increased PO_4^{3-} uptake rate under increasing light intensity (Perrin et al., 2016). On the other hand, several

studies report that ocean acidification and reduced phosphorus availability acted synergistically to increase the cellular POC content, especially at high light intensity, and acted antagonistically to affect cellular PIC content of *E. huxleyi* (Leonardos and Geider, 2005; Matthiessen et al., 2012; Zhang et al., 2020). In addition, ocean acidification normally amplified the positive effect of increasing light intensity on cellular POC content (Rokitta and Rost, 2012; Heidenreich et al., 2019). Due to high proton concentration-induced reduction in HCO_3^- uptake rate, ocean acidification could weaken or counteract the positive effect of increasing light intensity on cellular PIC content (Rokitta and Rost, 2012; Kottmeier et al., 2016). Overall, while recent studies have focused on physiological performance of *E. huxleyi* and their effects on marine biogeochemical cycling of carbon, little information is available about the biochemical response of *E. huxleyi* to reduced phosphorus availability, increasing light intensity and ocean acidification.

The objective of this study is to investigate the combined effects of reduced phosphorus availability, increasing light intensity and ocean acidification on cellular elemental contents, the carbon (C) : nitrogen (N) : phosphorus (P) ratio and macromolecules of *E. huxleyi*, and to analyze the effects of macromolecules on elemental contents. Under reduced phosphorus availability, increasing light intensity and ocean acidification, we hypothesize that increased cellular POC content is more likely to be caused by increased carbohydrate content. In addition, we discuss the potential mechanisms for changing cellular PIC content in response to changed levels of phosphate, light, and CO_2, which is important for projections of changes in coccolithophore biogeochemistry and ecology in the future ocean.

2 Materials and Methods

2.1 Experimental setup

Emiliania huxleyi strain RCC1266 (morphotype A) was originally isolated from shelf waters around Ireland (49°30' N, 10°30' W) in 2007 and obtained from the Roscoff algal culture collection (Fig. S1). *Emiliania huxleyi* was cultured under a 14 h : 10 h light : dark cycle (light period: 06:00 to 20:00 h) in a thermo-controlled incubator (MGC-400H, Shanghai Yiheng Scientific Instrument) at 20°C in semicontinuous cultures. The artifical seawater (ASW) media was prepared according to Berges et al. (2001) with a salinity of 33 psu, a boron concentration of 372 μmol L^{-1}, and with the addition of 2350 μmol L^{-1} bicarbonate to achieve the total alkalinity (TA) of 2350 μmol L^{-1}, and enriched with 64 μmol L^{-1} NO_3^-, f/8 concentrations for trace metals and vitamins (Guillard and Ryther, 1962). The experiment was conducted in two parts (Fig. S2). The first part (Part 1) was performed at 40 μmol photons m^{-2} s^{-1} (low light intensity, LL) and the second one (Part 2) was at 300 μmol photons m^{-2} s^{-1} (high light intensity, HL). The LL intensity used here corresponds to the lower end of the irradiance range of the UML, and the HL intensity represents to the irradiance in the surface ocean (Jin et al., 2016; Perrin et al., 2016). For each part of the experiment, dissolved inorganic phosphorus (DIP) concentration and ocean acidification were combined in a fully factorial design: high DIP concentration (4 μmol L^{-1})＋low CO_2 level (426 μatm, current CO_2 level) (HP+LC, treatment 1 in LL and treatment 5 in HL), high DIP concentration (4 μmol L^{-1})＋high CO_2 level (946 μatm, future CO_2 level) (HP+HC, treatment 2 in LL and treatment 6 in HL), low DIP concentration (0.43 μmol L^{-1})＋low CO_2 level (426 μatm) (LP+LC, treatment 3 in LL and treatment 7 in HL), and low DIP concentration (0.43 μmol L^{-1})＋high CO_2 level (946 μatm) (LP+HC, treatment 4 in LL and treatment 8 in HL). High DIP concentration is replete for physiological process of *E. huxleyi*, and at the end of the incubation, low DIP

176 concentration limits the growth of *E. huxleyi* (see below). There were eight treatments

177 totally and four biological replicates for each treatment (Fig. S2). In all cases, cell

178 densities were lower than 78,000 cells mL^{-1} and the cells were acclimated to each

179 treatment for at least 8 generations before physiological and biochemical parameters

180 were measured.

181   At LL intensity (Part 1), for the treatments of HP+LC and HP+HC, the ASW media

182 were enriched with 4 μmol L^{-1} PO_4^{3-} and aerated for 24 h at 20°C with filter-sterilized

183 (PTFE filter, 0.22 μm pore size, Nantong) air pumped from the room. The pH_{Total}

184 (total scale) values of the media under both HP+LC and HP+HC treatments were

185 about 8.04. The dry air was humidified with Milli-Q water prior to the aeration to

186 minimize evaporation. Under the HP+HC treatment, the pH_{Total} values of the media

187 were adjusted to 7.74 by stepwise additions of CO_2-saturated seawater. For the

188 treatments of LP+LC and LP+HC, the ASW media were enriched with 0.4 μmol L^{-1}

189 PO_4^{3-} and aerated for 24 h at 20°C with filtered room air. Under the LP+HC treatment,

190 the pH_{Total} values of the media were also adjusted to 7.74 as described above. The

191 HP+LC, HP+HC, LP+LC and LP+HC seawater were then filtered (0.22 μm pore size,

192 Polycap 75 AS, Whatman) and carefully pumped into autoclaved 50 mL (for TA

193 measurements), 600 mL (for pre-experimental cultures) and 2350 mL (for

194 experimental cultures) polycarbonate bottles (Nalgene) with no headspace to

195 minimize gas exchange. The cells were inoculated to achieve an initial density of

196 5000 cells ml^{-1} in the HP+LC and HP+HC conditions, respectively, and cultured for 2

197 days, then diluted to the initial density again. These processes were performed three

198 times in 600 mL bottles for pre-experimental cultures at 40 μmol photons m^{-2} s^{-1} (LL)

199 of photosynthetically active radiation (PAR; measured using a LI-190SA quantum

200 sensor, Beijing Ligaotai Technology Co. Ltd.). In the main experimental cultures, the

201 cells were transferred from 600 mL to 2350 mL bottles at the same time, and cultured

202 for another 2 days (Fig. S2b). Culture bottles were rotated 10 times until cells were

203 mixed at 09:00 h, 13:00 h and 19:00 h. In the second day of the main experimental

204 cultures, subsamples were taken for measurements of cell densities, pH_{Total}, TA,

205 cellular contents of total particulate carbon (TPC), particulate organic carbon (POC),

206 nitrogen (PON) and phosphorus (POP), carbohydrate and protein. At the end of the

207 cultures under the previous conditions, cell samples with an initial density of 5000

208 cells ml^{-1} were transferred from HP+LC condition (treatment 1) to LP+LC condition

209 (treatment 3), and from HP+HC condition (treatment 2) to LP+HC condition

210 (treatment 4) at LL intensity. The cells were acclimated to LP+LC and LP+HC

211 conditions for 8 generations before subsamples were taken for measurements, which

212 allows cells to have enough time periods to change growth rate against the low DIP

213 concentration.

214   At HL intensity (Part 2), samples grown under the HP+LC and HP+HC conditions

215 were transferred from 40 (LL) to 300 μmol photons m^{-2} s^{-1} (HL) of PAR with initial

216 cell density of 5000 cells ml^{-1}. The cells were cultured under the HP+LC and HP+HC

217 conditions for 2 days, respectively, and then diluted back to the initial cell density.

218 These processes were performed three times in 600 mL bottles at HL intensity, and

219 then the main experimental cultures were conducted in 2350 mL bottles. On the

220 second day of the incubation, subsamples were taken for measurements of the

221 parameters. After that, cell samples with an initial density of 5000 cells ml^{-1} were

222 transferred from HP+LC condition (treatment 5) to LP+LC condition (treatment 7),

223 and from HP+HC condition (treatment 6) to LP+HC condition (treatment 8). At HL

224 intensity, cell samples were acclimated for at least 8 generations in LP+LC and

225 LP+HC conditions, respectively, before subsamples were taken for measurements.

2.2 Phosphate concentration and carbonate chemistry measurements

In the beginning and on the second day of the incubations, samples for determinations of phosphate concentration (20 mL), pH_{Total} value (20 mL) and total alkalinity (TA) (50 mL) were, respectively, filtered (PTFE filter, 0.22 μm pore size, Nantong) 7 h after the onset of the light period (at 13:00). Dissolved inorganic phosphorus (DIP) concentration was measured using a spectrophotometer (SP-722, Shanghai Spectrum Instruments) following the phosphomolybdate method (Hansen and Koroleff, 1999). The bottle for pH measurement was filled from bottom to top with overflow and closed without a headspace. The pH_{Total} value was measured immediately at 20°C using a pH meter which was corrected with a standard buffer of defined pH in seawater (Dickson, 1993). TA samples were treated with 10 μL saturated $HgCl_2$ solution and stored in the dark at 4.0°C, and TA was measured at 20°C by potentiometric titration (AS-ALK1+, Apollo SciTech) according to Dickson et al. (2007). Carbonate chemistry parameters were estimated from TA and pH_{Total} using the CO2SYS program of Pierrot et al. (2006) with carbonic acid constants, K_1 and K_2, taken from Roy et al. (1993).

2.3 Cell density and elemental content measurements

Twenty milliliter samples to monitor the cell density were taken daily at 13:30 h, and fresh media with the same DIP concentration and carbonate chemistry as in the initial treatment conditions were added as top-up. Cell densities were determined using a Multisizer™3 Coulter Counter (Beckman Coulter). Growth rates were calculated for each replicate according to the equation: $\mu = (\ln N_t - \ln N_0) / d$, where N_t and N_0 refer to the cell densities on the second day and in the beginning of the main experiment,

251 respectively, and *d* was the growth period in days.

252   After mixing, samples for determinations of TPC (300 mL), POC and PON (300

253 mL), and POP (300 mL) were obtained by filtering onto GF/F filters (precombusted at

254 450°C for 6 h) at the same time (14:00 h) in each treatment. For POC and PON

255 measurements, samples were fumed with HCl for 12 h to remove inorganic carbon.

256 TPC, POC and PON samples were dried at 60°C for 12 h and analyzed using an

257 Elementar CHNS analyzer (Vario EL cube, GmbH, Germany). Cellular particulate

258 inorganic carbon (PIC) content was calculated as the difference between cellular TPC

259 and POC contents (Fabry and Balch, 2010). To remove dissolved inorganic

260 phosphorus from the GF/F filters, POP samples were rinsed three times with 0.17 mol

261 L^{-1} Na_2SO_4. After that, 2 mL 0.017 mol L^{-1} $MgSO_4$ solution was added onto filters,

262 and POP samples were dried at 90°C for 12 h, and then combusted at 500°C for 6 h to

263 remove POC and digested by 0.2 mol L^{-1} HCl (Solórzano and Sharp, 1980).

264 Phosphorus concentration was measured using a microplate reader (Thermo Fisher)

265 following the ammonium molybdate method (Chen et al., 1956) using

266 adenosine-5-triphosphate disodium trihydrate as a standard.

267

268 **2.4 Protein and carbohydrate measurements**

269 Samples for determinations of protein (600 mL) and carbohydrate (600 mL) were,

270 respectively, filtered onto polycarbonate filters (0.6 μm pore size, Nuclepore,

271 Whatman) and onto precombusted GF/F filters at 14:30 h. Protein samples were

272 extracted by bead milling (FastPrep Lysing Matrix D) in 0.5 mL 1× protein extraction

273 buffer (lithium dodecyl sulfate, ethylene diamine tetraacetic acid, Tris, glycerol and

274 4-(2-aminoethyl) benzenesulfonyl fluoride hydrochloride). Bead milling was

275 performed four times for 1 min at 6.5 ms^{-1}, and samples were placed on ice for 2 min

between each round of bead milling to prevent degradation. The samples were then centrifuged at $10,000 \times g$ for 5 min (Centrifuge 5418 R, Eppendorf, Germany), and extracted protein in the supernatant was quantified using the BCA assay with bovine gamma globulin as a standard using a microplate reader (Ni et al., 2016). Carbohydrate samples were hydrolyzed with 12.00 mol L^{-1} H_2SO_4 in the dark for 1 h and diluted by Milli-Q water to a final H_2SO_4 concentration of 1.20 mol L^{-1}. Then, samples were sonicated for 5 min, vortexed for 30 s, and boiled at 90^oC for 3 h (Pakulski and Benner, 1992). The extracted carbohydrate was determined by phenol sulfuric reaction with D–glucose as standard (Masuko et al., 2005).

2.5 Data analysis

The percentages of carbon (C : carbohydrate is 40% and C : protein is 53%) and nitrogen (N : protein is 16%) contributed by carbohydrate and protein were calculated from the elemental composition of biochemical classes compiled by Geider and LaRoche (2002). A three-way ANOVA was used to determine the main effects of DIP concentration, light intensity and CO_2 level, and their interactions on each variable. A Tukey post hoc test was performed to identify significant differences between two DIP concentrations, two light intensities and two CO_2 levels. A Shapiro–Wilk test was conducted to analyze the normality of residuals and a Levene test was conducted graphically to test for homogeneity of variances. The significant difference between treatments was set at $p < 0.05$. All data analyses were conducted using the statistical software R with the packages carData, lattice and nlme (R version 3.5.0).

3 Results

3.1 Dissolved inorganic phosphorus concentration and carbonate chemistry

301 **parameters**

302 During the incubations, organismal activity significantly reduces dissolved inorganic

303 phosphorus (DIP) concentrations (Table 1). Under high phosphorus (HP) treatment,

304 DIP concentrations decrease by 20.32% in low light (LL) and low CO_2 (LC), by

305 22.32% in LL and high CO_2 (HC), by 27.66% in high light (HL) and LC, and by

306 31.58% in HL and HC. Under low phosphorus (LP) treatment, DIP concentrations

307 decrease from 0.43 μmol L^{-1} at the beginning of the experiment to be lower than 0.04

308 μmol L^{-1} (the detection limit) at the end of the incubation in LL and LC conditions, in

309 LL and HC conditions, in HL and LC conditions, and in HL and HC conditions.

310 During the incubations, at LL intensity, pH_T values increase by, on average, 0.02 in

311 HP+LC, by 0.03 in HP+HC, by 0.09 in LP+LC, and by 0.10 in LP+HC conditions

312 (Table 1). At HL intensity, pH_T values increase by 0.05 in HP+LC, by 0.06 in HP+HC,

313 by 0.12 in LP+LC, and by 0.09 in LP+HC conditions. Correspondingly, at LL

314 intensity, seawater CO_2 concentrations decrease by 5.53% in HP+LC, by 6.89% in

315 HP+HC, by 22.76% in LP+LC, and by 22.77% in LP+HC. At HL intensity, seawater

316 CO_2 concentrations decrease by 16.18% in HP+LC, by 16.41% in HP+HC, by

317 28.92% in LP+LC, and by 22.30% in LP+HC. Overall, organismal activity has larger

318 effects on carbonate chemistry under the LP treatment than under the HP treatment.

319

320 **3.2 Growth rate**

321 The effect of increasing light intensity on growth rate is positive which can be seen by

322 comparing growth rate in the HL regimes with their paired LL regimes (Fig. 1a; Table

323 2), though the extent of increase in growth rate depends on CO_2 levels and phosphate

324 availability. Compared to LL intensity, growth rates at HL intensity increased by

325 48.48% in HP+LC, by 50.87% in HP+HC, by 60.86% in LP+LC, and by 60.80% in

326 LP+HC (Tukey post hoc test, all values of $p < 0.01$). The effect of increasing CO_2

327 levels on growth rate depends on light intensity and phosphate availability (Fig. 1a).

328 Compared to LC level, growth rates in HC level decreased by 3.08% in LL and HP

329 condition ($p = 0.48$), by 16.13% in LL and LP condition ($p < 0.01$), by 1.50% in HL

330 and HP condition ($p = 0.68$), and by 16.27% in HL and LP condition ($p < 0.01$). The

331 effect of reduced phosphorus availability on growth rate is negative and the extent of

332 reduction in growth rate depends on light intensity and CO_2 levels (Fig. 1a).

333 Compared to HP availability, growth rates in LP availability decreased by 8.46% in

334 LL and LC condition ($p < 0.01$), by 20.81% in LL and HC condition ($p < 0.01$), and by

335 15.63% in HL and HC condition ($p < 0.01$), and did not change significantly in HL

336 and LC condition ($p = 0.99$). These results show that high CO_2 levels and low

337 phosphorus availability acted synergistically to reduce growth rate of *E. huxleyi*, and

338 increasing light intensity could partly counteract this response (Table S1).

339

3.3 Cellular POC, PON, POP and PIC contents

341 The effect of increasing light intensity on cellular POC content is positive, which was

342 observed by comparing POC content in all the HL regimes with their paired LL

343 regimes (Fig. 1b). The extent of increase in POC content depends on CO_2 levels and

344 phosphate availability. Compared to LL intensity, cellular POC contents at HL

345 intensity increased by 27.15% in HP+LC, by 26.51% in HP+HC, by 43.24% in

346 LP+LC, and by 58.13% in LP+HC conditions (Tukey post hoc test, all values of $p <$

347 0.01). The effect of increasing CO_2 levels on POC content is light and phosphate

348 dependent and can be seen by comparing POC content in the HC regimes with their

349 paired LC regimes (Fig. 1b). At LL intensity, cellular POC contents are not

350 significantly different between HP+LC, HP+HC, LP+LC and LP+HC conditions (all

351 values of $p > 0.1$). At HL intensity, compared to LC level, cellular POC contents in

352 HC level increased by 5.12% in HP condition ($p = 0.74$), and by 8.28% in LP

353 condition ($p = 0.07$). The effect of phosphate reduction on POC content is light and

354 CO_2 dependent, which can be seen by comparing POC content in the LP regimes with

355 those in their paired HP regimes (Fig. 1b). At LL intensity, cellular POC contents did

356 not significantly differ between LP and HP availability. At HL intensity, compared to

357 HP availability, cellular POC contents in LP availability increased by 11.80% in LC

358 condition ($p = 0.02$), and by 15.28% in HC condition ($p < 0.01$). These results show

359 that ocean acidification and reduced phosphorus availability acted synergistically to

360 increase POC contents in HL condition but not in LL condition (Table S1).

361   The effect of increasing light intensity on cellular PON content depends on CO_2

362 levels and phosphate availability (Fig. 1c). Compared to LL intensity, cellular PON

363 contents at HL intensity increased by 12.03% in HP+LC condition ($p = 0.27$), by

364 19.54% in HP+HC condition ($p < 0.01$), by 22.68% in LP+LC condition ($p < 0.01$),

365 and by 30.90% in LP+HC condition ($p < 0.01$). The effect of increasing CO_2 levels on

366 PON content is light and phosphate dependent, which can be seen by comparing POC

367 content in the HC regimes with their paired LC regimes (Fig. 1c). Compared to LC

368 level, cellular PON contents in HC level did not change significantly in LL and HP

369 condition, in LL and LP condition, in HL and LP condition, and increased by 14.68%

370 in HL and HP condition ($p = 0.02$). The effect of phosphate reduction on PON content

371 is CO_2 and light dependent, which can be seen by comparing PON content in the LP

372 regimes with those in their paired HP regimes (Fig. 1c). Compared to HP availability,

373 cellular PON contents in LP availability decreased by 16.59% in LL and LC condition

374 ($p = 0.01$), by 24.03% in LL and HC condition ($p < 0.01$), by 8.35% in HL and LC

375 condition ($p = 0.43$), and by 17.32% in HL and HC condition ($p < 0.01$). These results

376   show that increasing light intensity compensated for the negative effect of phosphate

377   reduction on PON content (Table S1).

378   The effect of increasing light intensity on POP content is positive and can be seen

379   by comparing POP content in the HL regimes with their paired LL regimes, though

380   the extent of increase in POP content depends on CO_2 levels and phosphate

381   availability (Fig. 1d). Compared to LL intensity, cellular POP contents at HL intensity

382   increased by 35.79% in HP+LC, by 41.70% in HP+HC, by 57.22% in LP+LC, and by

383   56.44% in LP+HC conditions (Tukey post hoc test, all values of $p < 0.01$). Ocean

384   acidification did not change the POP contents significantly under all treatments used

385   here (all values of $p > 0.53$) (Fig. 1d). Reduced phosphorus availability significantly

386   decreased the POP contents, which can be seen by comparing POP content in the LP

387   regimes with their paired HP regimes, though the extent of reduction in POP content

388   depends on light intensity and CO_2 levels (Fig. 1d). Compared to HP availability,

389   cellular POP contents in LP availability decreased by 52.96% in LL and LC condition,

390   by 54.03% in LL and HC condition, by 46.11% in HL and LC condition, and by

391   49.51% in HL and HC condition (all values of $p < 0.01$). These results show that

392   reduced phosphorus availability had a larger effect on POP content than that of ocean

393   acidification and increasing light intensity (Table S1).

394   The effect of increasing light intensity on PIC content is positive, which can be

395   seen by comparing PIC content in the HL regimes with their paired LL regimes,

396   though the extent of increase in PIC content depends on CO_2 levels and phosphorus

397   availability (Fig. 1e). Compared to LL intensity, cellular PIC contents at HL intensity

398   increased by 77.87% in HP+LC, by 70.28% in HP+HC, by 98.31% in LP+LC, and by

399   90.68% in LP+HC conditions (Tukey post hoc test, all values of $p < 0.01$). The effect

400   of increasing CO_2 levels on PIC content is negative and can be seen by comparing

PIC content in the HC regimes with those in their paired LC regimes (Fig. 1e). The extent of reduction in PIC content depends on light intensity and phosphorus availability. Compared to LC level, cellular PIC contents under ocean acidification decreased by 31.43% in LL and HP condition ($p = 0.09$), by 16.00% in LL and LP condition ($p = 0.67$), by 35.02% in HL and HP condition ($p < 0.01$), and by 21.12% in HL and LP condition ($p < 0.01$). The effect of phosphate reduction on PIC content is positive which can be seen by comparing PIC content in the LP regimes with their paired HP regimes, though the extent of increase in PIC content depends on light intensity and CO_2 levels (Fig. 1e). Compared to HP availability, cellular PIC contents in LP availability increased by 16.00% in LL and LC condition ($p = 0.83$), by 41.26% in LL and HC condition ($p = 0.16$), by 29.98% in HL and LC condition ($p < 0.01$), and by 60.44% in HL and HC condition ($p < 0.01$). These results show that high light intensity and low phosphorus availability acted synergistically to increase PIC content, which counteracts the negative effect of ocean acidification on PIC content (Table S1).

3.4 Carbohydrate and protein contents

The effect of increasing light intensity on carbohydrate content is positive and can be seen by comparing carbohydrate content in the HL regimes with their paired LL regimes, though the extent of increase in carbohydrate depends on CO_2 levels and phosphorus availability (Fig. 2a). Compared to LL intensity, cellular carbohydrate contents at HL intensity increased by 148.81% in HP+LC condition, by 139.42% in HP+HC condition, by 179.12% in LP+LC condition, and by 204.42% in LP+HC condition (all values of $p < 0.01$). The effect of increasing CO_2 levels on carbohydrate content is light and phosphate dependent which can be seen by comparing

426 carbohydrate content in the HC regimes with their paired LC regimes (Fig. 2a).

427 Compared to LC level, cellular carbohydrate contents under ocean acidification did

428 not change significantly under LL condition, and increased by 21.32% in HL and HP

429 condition ($p = 0.02$), and by 18.45% in HL and LP condition ($p < 0.01$). The effect of

430 phosphate reduction on carbohydrate content is light and CO_2 dependent and can be

431 seen by comparing carbohydrate content in the LP regimes with their paired HP

432 regimes (Fig. 2a). Compared to HP availability, cellular carbohydrate contents in LP

433 availability did not change significantly in LL and LC condition, in LL and HC

434 condition (both $p > 0.65$) and increased by 40.13% in HL and LC condition ($p < 0.01$),

435 and by 36.00% in HL and HC condition ($p < 0.01$). These results show that increasing

436 light intensity dominantly increased carbohydrate content, and ocean acidification and

437 reduced phosphorus availability acted synergistically to increase carbohydrate

438 contents under high light intensity (Table S1).

439 The effect of increasing light intensity on cellular protein content is positive, which

440 can be seen by comparing protein content in the HL regimes with their paired LL

441 regimes, though the extent of increase in protein content depends on CO_2 level and

442 phosphorus availability (Fig. 2b). Compared to LL intensity, cellular protein contents

443 at HL intensity increased by 24.76% in HP+LC condition, by 30.43% in HP+HC

444 condition, by 68.09% in LP+LC condition, and by 65.39% in LP+HC condition (all

445 values of $p < 0.01$). The effect of increasing CO_2 levels on protein content can be seen

446 by comparing protein content in the HC regimes with their paired LC regimes (Fig.

447 2b). Compared to LC level, cellular protein contents under ocean acidification did not

448 change significantly in LL and HP condition, in LL and LP condition, in HL and HP

449 condition, and in HL and LP condition (all values of $p > 0.09$). The effect of

450 phosphate reduction on protein content is light and CO_2 dependent, which can be seen

by comparing protein content in the LP regimes with their paired HP regimes (Fig. 2b). Compared to HP availability, cellular protein content in LP availability decreased by 27.88% in LL and LC condition, by 28.80% in LL and HC condition (both $p < 0.01$) and did not change significantly in HL and LC condition, and in HL and HC condition (both $p > 0.11$). These results show that high light intensity counteracted the negative effect of low phosphorus availability on protein content, and ocean acidification had less effect on protein content (Table S1).

3.5 Percentage of POC allocated to carbohydrate (carbohydrate–C : POC) and protein (protein–C : POC)

Increasing light intensity increased the percentage of POC allocated to carbohydrate (carbohydrate–C : POC), which can be seen by comparing carbohydrate–C : POC in the HL regimes with their paired LL regimes, though the extent of increase in carbohydrate–C : POC depends on CO_2 levels and phosphorus availability (Fig. 2c). Compared to LL intensity, carbohydrate–C : POC at HL intensity increased by 95.60% in HP+LC condition, by 97.69% in HP+HC condition, by 95.05% in LP+LC condition, and by 83.37% in LP+HC condition (all values of $p < 0.01$). The effect of increasing CO_2 levels on carbohydrate–C : POC is light and phosphate dependent, and can be seen by comparing carbohydrate–C : POC in the HC regimes with their paired LC regimes (Fig. 2c). Compared to LC level, carbohydrate–C : POC under ocean acidification increased by 20.12% in LL and HP condition, by 11.42% in LL and LP condition, by 20.36% in HL and HP condition, and by 4.40% in HL and LP condition (all values of $p > 0.08$). The effect of phosphate reduction on carbohydrate–C : POC is light and CO_2 dependent, which can be seen by comparing carbohydrate–C : POC in the LP regimes with those in their paired HP regimes (Fig. 2c). Compared to HP

476 availability, carbohydrate–C : POC in LP availability increased by 25.61% in LL and

477 LC condition ($p = 0.16$), by 17.37% in LL and HC condition ($p = 0.47$), by 25.81% in

478 HL and LC condition ($p < 0.01$), and by 8.11% in HL and HC condition ($p < 0.05$).

479 These results show that increasing light intensity, ocean acidification and reduced

480 phosphorus availability acted synergistically to increase the percentage of POC

481 allocated to carbohydrate (Table S1).

482   Increasing light intensity did not significantly change the percentage of POC

483 allocated to protein (protein–C : POC) under the phosphorus availability and CO_2

484 levels used here (Fig. 2d). Ocean acidification did not significantly affect the

485 protein–C : POC in LL and HP, in LL and LP, in HL and HP, and in HL and LP

486 conditions. The effect of phosphate reduction on protein–C : POC is light and CO_2

487 dependent, which can be seen by comparing the protein–C : POC in the LP regimes

488 with their paired HP regimes (Fig. 2d). Compared to HP availability, protein–C : POC

489 in LP availability decreased by 27.39% in LL and LC condition ($p < 0.01$), by 23.05%

490 in LL and HC condition ($p < 0.01$), by 12.81% in HL and LC condition ($p = 0.09$),

491 and by 21.77% in HL and HC condition ($p < 0.01$). These results show that reduced

492 phosphorus availability dominantly reduced the protein–C : POC, and increasing light

493 intensity and ocean acidification had less effects on protein–C : POC (Table S1). On

494 the other hand, increasing light intensity, reduced phosphorus availability and ocean

495 acidification did not significantly change the percentage of PON allocated to protein

496 (protein–N : PON) (Fig. 2e).

497

498 **3.6 Elemental stoichiometry and protein content as a function of growth rate**

499 Reduced phosphorus availability increased the POC : PON ratio, and the extent of the

500 increase was larger under HL than LL intensity (Fig. S5a). At LL and HL intensities,

both POC : POP ratio and PON : POP ratio were linearly and negatively correlated

with growth rates (Fig. 3a,b). In LL and HL conditions, POC : POP ratio decreased

linearly with increasing growth rate ($R^2 = 0.71$, $F = 32.08$, $p < 0.01$ in LL condition;

$R^2 = 0.53$, $F = 14.63$, $p < 0.01$ in HL condition). Similarly, in LL and HL conditions,

PON : POP ratio decreased linearly with increasing growth rate ($R^2 = 0.69$, $F = 29.23$,

$p < 0.01$ in LL condition; $R^2 = 0.50$, $F = 13.31$, $p < 0.01$ in HL condition). In all

treatments, protein content increased linearly with increasing growth rate ($R^2 = 0.76$,

$F = 151.14$, $p < 0.01$) (Fig. 3c), and POC content increased linearly with increasing

carbohydrate content ($R^2 = 0.94$, $F = 435.10$, $p < 0.01$) (Fig. 3d).

4 Discussion

Coccolithophores play a complex role in the marine carbon cycle through production

and export of organic carbon to depth but also through the carbonate counter pump,

and their responses to global climate change could have significant consequences for

marine carbon cycling (Riebesell et al., 2017). The bloom-forming coccolithophore *E.*

huxleyi, dominating the assemblages in seawater under limited phosphorus condition,

is likely to be exposed to increasing light intensity and ocean acidification in the

future ocean (Kubryakova et al., 2021). In this study, we observed that increasing

light intensity compensates for the negative effects of low phosphorus availability on

cellular protein and nitrogen contents (Figs. 1 and 2). Reduced phosphorus

availability, increasing light intensity and ocean acidification act synergistically to

increase cellular contents of carbohydrate and POC, and the allocation of POC to

carbohydrate. These changes in *E. huxleyi* could provide vital information for

evaluating carbon cycle in marine ecosystems under global change.

Ribonucleic acid (RNA) is the main phosphorus-containing macromolecule within

the cell (Geider and La Roche, 2002). Therefore, the reduced phosphorus availability dominantly reduces the RNA content (Fig. S6), which contributes to low POP contents (McKew et al., 2015) (Fig. 1d). In eukaryotic cells, ribosomal RNA (rRNA) constitutes about 80% of the total RNA and is mainly used to create ribosome (Dyhrman, 2016). Thus, reduced RNA contents decrease the numbers of ribosome, which has a potential to decrease protein synthesis (Dyhrman, 2016; Rokitta et al., 2016). On the other hand, the separation of the regression line between POC : POP ratio (or PON : POP ratio) and growth rate under low and high light intensities suggests different POP storage contents in *E. huxleyi* among different light intensities (Perrin et al., 2016). Low light intensity down-regulates the expression of genes related to nitrate reductase and nitrite reductase, and then reduces the nitrate uptake and assimilation efficiency of *E. huxleyi* and other phytoplankton species (Perrin et al., 2016; Lu et al., 2018), which exacerbates the negative effect of low phosphorus availability on protein synthesis and PON contents (Figs. 1c and 2b). Besides that, low light intensity significantly reduces the rates of RNA synthesis, carbohydrate synthesis and cell division (Zhang et al., 2021), which adds to the negative effect of low phosphorus availability on growth rate of *E. huxleyi* (Fig. 1a). Under high light intensity and low CO_2 level, reduced phosphorus availability did not change growth rate and protein content (Figs. 1a and 2b), which suggests that *E. huxleyi* might compensate for low phosphate-induced decreases in ribosome content by increasing protein synthesis efficiency under increasing light intensity (Reith and Cattolico, 1985). Under high light intensity and ocean acidification, reduced phosphorus availability did not significantly change cellular protein content while reduced growth rate, which might indicate the lowered protein synthesis efficiency (McKew et al., 2015).

551   Several studies report that reduced phosphorus availability (0.4–0.5 µmol L^{-1}) did

552   not change growth rates significantly during the short-time (2 or 3 days) incubations

553   under low CO_2 level and high light intensity (Rokitta et al., 2016; Zhang et al., 2020;

554   Wang et al., 2022). The reasons could be that *E. huxleyi* cells developed high affinity

555   for phosphate and increased the uptake rate of phosphate (Wang et al., 2022) and

556   could replace the phospholipid membrane with non-phosphorus membrane during the

557   short-time incubation of phosphorus limitation (Shemi et al., 2016). Our data showed

558   that reduced phosphorus availability and ocean acidification acted synergistically to

559   reduce growth rate under both low and high light intensities (Fig. 1a). One of the

560   reasons could be that low pH value under ocean acidification up regulates the

561   expressions of a series of genes involved in ribosome metabolism, such as genes of

562   large subunit ribosomal protein L3, L38E, L30E (*RP-L3*, *RP-L38E*, *RP-L30E*), and

563   small subunit ribosomal protein S3E, S5E, SAE (*PR-S3E*, *PR-S5E*, *RP-SAE*) in *E.*

564   *huxleyi* (Wilson and Doudna Cate, 2012) (Fig. S7). Under ocean acidification, up

565   regulation of expression of these genes has the potential to drive cells to allocate more

566   phosphorus to synthesize ribosome, and to reduce the allocation of phosphorus to

567   DNA replication (Rokitta et al., 2011), which exacerbates the limitation of reduced

568   phosphorus availability on the rate of cell division in *E. huxleyi* (Rouco et al., 2013).

569   Under phosphorus-replete condition, more phosphorus is reallocated to ribosome

570   metabolism under ocean acidification which could facilitate nitrogen assimilation (Fig.

571   2b). Overall, under high light intensity, ocean acidification is likely to facilitate *E.*

572   *huxleyi* cells to increase nitrogen content in phosphorus-replete condition and to

573   reduce growth rate in phosphorus-limitation.

574   In this study, we found that low light intensity dominantly limits carbon

575   assimilation of *E. huxleyi* and reduces the effects of phosphate availability and ocean

576 acidification on cellular carbohydrate and POC contents (Figs. 1b and 2a). However,

577 under high light intensity, *E. huxleyi* had high carbohydrate and POC contents while

578 low growth rate under reduced phosphorus availability and ocean acidification (Figs.

579 1a,b and 2a), which suggests that carbon assimilation rate did not change significantly

580 while cell division rate decreased (Matthiessen et al., 2012; Perrin et al., 2016).

581 Furthermore, carbohydrate is a carbon- and energy-storing macromolecule, and

582 protein is related to growth rate (Geider and La Roche, 2002). Under high light

583 intensity, reduced phosphorus availability and ocean acidification, *E. huxleyi* cells

584 could synthesize more carbohydrate to store carbon and energy but didn't increase

585 protein content, which contributes to the large percentage of POC allocated to

586 carbohydrate (Fig. 2c).

587 The physiological reasons for reduced calcification rate under ocean acidification

588 could be due to high proton concentration-induced reduction in HCO_3^- uptake rate

589 (Meyer and Riebesell, 2015; Kottmeier et al., 2016). The molecular mechanisms for

590 low PIC content under ocean acidification may be due to down-regulation of a series

591 of genes potentially involved in ion transport and pH regulation, such as genes of

592 calcium/proton exchanger (*CAX3*), sodium/proton exchanger (*NhaA2*) and

593 membrane-associated proton pump (*PATP*) (Mackinder et al., 2011; Lohbeck et al.,

594 2014). On the other hand, increasing light intensity up-regulates a series of genes

595 related to ion transport, such as gene of *CAX3*, gene of Cl^-/HCO_3^- exchanger and

596 genes of various subunits of a vacuolar H^+–ATPase (*V–ATPase*) and so on (Rokitta et

597 al., 2011). Up-regulation of these genes in high light intensity has the potential to

598 facilitate cells to take up HCO_3^- and Ca^{2+}, and to pump proton outside the cells, and

599 then leads to large PIC content of *E. huxleyi* (Kottmeier et al., 2016). Our data suggest

600 that increasing light intensity counteracts the negative effect of ocean acidification on

cellular PIC content of *E. huxleyi* (Fig. 1e). These results are consistent with the findings of Feng et al. (2020) who reported that combinations of increasing light intensity and ocean acidification increase the expression of genes involved in calcium-binding proteins (*CAM* and *GPA*), which has the potential to increase calcium influx into cells and then compensate for the effect of reduced HCO_3^- uptake rate on calcification. It is also suggested that increasing light intensity could cause cells to remove H^+ faster which neutralizes the effect of high proton concentration on calcification (Jin et al., 2017). On the other hand, reduced phosphorus availability extends the G1 phase of cell cycle where calcification occurs, which prolongs the calcification time and then increases cellular PIC content (Müller et al., 2008). In addition, reduced phosphorus availability up-regulates expressions of genes of Ca^{2+} uptake, proton removal and carbonic anhydrase, and then increases coccolith production (Wang et al., 2022), which contribute to a larger PIC content and counteract the negative effect of ocean acidification on PIC contents (Borchard et al., 2011) (Fig. 1e). Furthermore, one of the reasons for larger PIC contents under reduced phosphorus availability and increasing light intensity conditions are likely due to larger and more numerous coccoliths (Gibbs et al., 2013; Perrin et al., 2016). Overall, responses of calcification of *E. huxleyi* to ocean climate change are complex than previously thought (Meyer and Riebesell, 2015), and it is worth exploring the underlying mechanisms of calcification under changing multiple environmental drivers (Mackinder et al., 2011; Feng et al., 2020).

Cellular POP content of *E. huxleyi* generally decreased, and POC : POP ratio and PON : POP ratio increased with reducing phosphorus availability (Leonardo and Geider, 2005; McKew et al., 2015). The negative correlations between growth rate and POC : POP ratio or PON : POP ratio under each light intensity are consistent with

the growth rate hypothesis (Fig. 3), which proposes that growth rate increases with increasing RNA : protein ratio. Phosphorus in RNA accounts for a high percentage of total POP, whereas nitrogen in protein is the main form of PON (Zhang et al., 2021), and the growth rate hypothesis suggests that growth rate could increase with decreasing POC : POP ratio or PON : POP ratio (Sterner and Elser, 2002). Our results suggest that *E. huxleyi* could reallocate chemical elements and energy to synthesize carbohydrate, protein and RNA efficiently, and then regulate its elemental stoichiometry and growth rate to acclimate to reduced phosphorus availability, ocean acidification and increasing light intensity (Moreno and Martiny, 2018).

In the future ocean, large carbohydrate and POC contents, POC : PON ratio, and POC : POP ratio of coccolithophores indicate increases in carbon export to the deep ocean that may affect the efficiency of the biological carbon pump and the marine biogeochemical cycle of carbon (Meyer and Riebesell, 2015). In addition, increased cellular PIC content under phosphorus limitation condition may have the potential to weaken CO_2 uptake of the oceans in phosphorus-limited marine environments. In summary, responses of coccolithophores to climate change is likely to affect the marine carbon cycle in the future (Riebesell et al., 2017).

651

652

653

Data availability. The data are available upon request to the corresponding author (yongzhang@fjnu.edu.cn).

656

Author contributions. YZ (yongzhang@fjnu.edu.cn), ZL and KX contributed to the design of the experiment. YZ (yongzhang@fjnu.edu.cn), YZ (qsx20211022@student.fjnu.edu.cn), SM, HC and RH performed this experiment and biochemical analyses. YZ (yongzhang@fjnu.edu.cn) wrote the first manuscript draft. All authors contributed to the data analyses and editing of the paper.

662

Competing interests. The authors declare that they have no conflict of interest.

664

Acknowledgments. We would like to thank Professor Zoe V. Finkel for providing the *Emiliania huxleyi* RCC1266, Dr. Vinitha Ebenezer for her helpful revision of the manuscript, and Dr. Peng Jin and two anonymous reviewers for their helpful suggestions which have help us to improve the manuscript. This work was supported by the National Natural Science Foundation of China (41806129 [YZ], 32001180 [ZKL]).

671

672

673

674

675

676 **References**

677 Beaufort, L., Couapel, M., Buchet, N., Claustre, H., and Goyet, C.: Calcite production

678   by coccolithophores in the southeast Pacific Ocean, Biogeosciences, 5,

679   1101–1117, doi:10.5194/bg-5-1101-2008, 2008.

680 Berges, J. A., Franklin, D. J., and Harrison, P. J.: Evolution of an artificial seawater

681   medium: improvements in enriched seawater, artificial water over the past two

682   decades, J. Phycol., 37, 1138–1145, doi: 10.1046/j.1529-8817.2001.01052.x,

683   2001.

684 Borchard, C., Borges, A. V., Händel, N., and Engel, A.: Biogeochemical response of

685   *Emiliania huxleyi* (PML B92/11) to elevated CO_2 and temperature under

686   phosphorus limitation: A chemostat study, J. Exp. Mar. Biol. Ecol., 410, 61–71,

687   doi: 10.1016/j.jembe.2011.10.004, 2011.

688 Caldeira, K., and Wickett, M. E.: Oceanography: anthropogenic carbon and ocean pH,

689   Nature, 425, 365, doi: 10.1038/425365a, 2003.

690 Chen, P., Toribara, T. T., and Warner, H.: Microdetermination of phosphorus, Anal.

691   Chem., 28, 1756–1758, doi: 10.1021/ac60068a036, 1956.

692 Dickson, A. G., Sabine, C. L., and Christian, J. R.: Guide to best practice for ocean

693   CO_2 measurements, PICES Special Publication 3, pp. 191, 2007.

694 Dickson, A. G.: pH buffers for seawater media based on the total hydrogen ion

695   concentration scale, Deep-Sea Res., 40, 107–118, doi:

696   10.1016/0967-0637(93)90055-8, 1993.

697 Dyhrman, S. T.: Nutrients and their acquisition: phosphorus physiology in microalgae,

698   in: The physiology of microalgae, edited by: Borowitzka, M. A., Beardall, J. and

699   Raven, J. A., Springer, Heidelberg, 155–183, doi: 10.1007/978-3-319-24945-2,

700   2016.

701   Fabry, V. J., and Balch, W. M.: Direct measurements of calcification rates in

702   planktonic organisms, in: Guide to best practices for ocean acidification research

703   and data reporting, edited by: Riebesell, U., Fabry, V. J., Hansson, L. and

704   Gattuso, J. P., Luxembourg, Publications Office of the European Union, p.

705   201–212, doi: 10.2777/66906, 2010.

706   Feng, Y. Y., Roleda, M. Y., Armstrong, E., Summerfield, T. C., Law, C. S., Hurd, C.

707   L., and Boyd, P. W.: Effects of multiple drivers of ocean global change on the

708   physiology and functional gene expression of the coccolithophore *Emiliania*

709   *huxleyi*, Glob. Chang. Biol., 26, 5630–5645, doi: 10.1111/GCB.15259, 2020.

710   Gao, K., Beardall, J., Häder, D. P., Hall-Spencer, J. M., Gao, G., and Hutchins, D. A.:

711   Effects of ocean acidification on marine photosynthetic organisms under the

712   concurrent influences of warming, UV radiation, and deoxygenation, Front. Mar.

713   Sci., 6, 322, https://doi.org/10.3389/fmars.2019.00322, 2019.

714   Geider, R. J., and LaRoche, J.: Redfield revisited: variability of C:N:P in marine

715   microalgae and its biochemical basis, Eur. J. Phycol., 37, 1–17, doi:

716   10.1017/S0967026201003456, 2002.

717   Gibbs, S. J., Poulton, A. J., Brown, P. R., Daniels, C. J., Hopkins, J., Young, J. R.,

718   Jones, H. L., Thiemann, G. J., O'Dea, S. A., and Newsam, C.: Species-specific

719   growth response of coccolithophores to Palaeocene − Eocene environmental

720   change, Nat. Geosci., 6, 218–222, doi: 10.1038/ngeo1719, 2013.

721   Guillard, R. R. L., and Ryther, J. H.: Studies of marine planktonic diatoms. I.

722   Cyclotella nana Hustedt and Detonula confervacea Cleve, Can. J. Microbiol., 8,

723   229–239, doi: 10.1139/m62-029, 1962.

724   Hansen, H. P., and Koroleff, F.: Determination of nutrients, in: Methods of seawater

725   analysis, edited by: Grasshoff, K., Kremling, K. and Ehrhardt, M., WILEY-VCH

726   Publishers, ISBN: 3-527-29589-5, 1999.

727   He, S., Le, C., He, J., and Liu, N.: Empirical algorithm for detecting coccolithophore

728   blooms through satellite observation in the Barents Sea, Remote Sens. Environ.,

729   270, 112886, doi: 10.1016/j.res.2021.112886, 2022.

730   Heidenreich, E., Wördenweber, R., Kirschhöfer, F., Nusser, M., Friedrich, F., Fahl, K.,

731   Kruse, O., Rost, B., Franzreb, M., Brenner-Weiß, G., and Rokitta, S.: Ocean

732   acidification has little effect on the biochemical composition of the

733   coccolithophore *Emiliania huxleyi*, PLoS One, 14, e0218564, doi:

734   10.1371/journal.pone.0218564, 2019.

735   Jin, P., Gao, G., Liu, X., Li, F., Tong, S., Ding, J., Zhong, Z., Liu,N., and Gao, K.:

736   Contrasting photophysiological characteristics of phytoplankton assemblages in

737   the Northern South China Sea, PLoS ONE, 11, e0153555, doi:

738   10.1371/journal.pone.0153555, 2016.

739   Jin, P., Ding, J. C., Xing, T., Riebesell, U., and Gao, K. S.: High levels of solar

740   radiation offset impacts of ocean acidification on calcifying and non-calcifying

741   strains of *Emiliania huxleyi*, Mar. Ecol. Prog. Ser., 568, 47–58, doi:

742   10.3354/meps12042, 2017.

743   Jordan, R. W., and Winter, A: Assemblages of coccolithophorids and other living

744   microplankton off the coast of Puerto Rico during January–May 1995, Mar.

745   Micropaleontol., 39, 113–130, doi: 10.1016/S0377-8398(00)00017-7, 2000.

746   Kondrik, D. V., Pozdnyakov, D. V., and Johannessen, O. M.: Satellite evidence that *E.*

747   *huxleyi* phytoplankton blooms weaken marine carbon sinks, Geophys. Res. Lett.,

748   45, e2017GL076240, doi: 10.1002/2017GL076240, 2018.

749   Kottmeier, D. M., Rokitta, S. D., and Rost, B.: Acidification, not carbonation, is the

750   major regulator of carbon fluxes in the coccolithophore *Emiliania huxleyi*, New

Phytol., 211, 126–137, doi: 10.1111/nph.13885, 2016.

Kubryakova, E. A., Kubryakov, A. A., and Mikaelyan, A. S.: Winter coccolithophore blooms in the Black Sea: Interannual variability and driving factors, J. Mar. Syst., 213, 103461, doi: 10.1016/j.jmarsys.2020.103461, 2021.

Leonardos, K., and Geider, R. J.: Elevated atmospheric carbon dioxide increases organic carbon fixation by *Emiliania huxleyi* (haptophyta), under nutrient-limited high-light conditions, J. Phycol., 41, 1196–1203, doi: 10.1111/j.1529-8817.2005.00152.x, 2005.

Lohbeck, K., Riebesell, U., and Reusch, T. B. H.: Gene expression changes in the coccolithophore *Emiliania huxleyi* after 500 generation of selection to ocean acidification, Proc. R. Soc. B., 281, 20140003, doi: 10.1098/rspb.2014.0003, 2014.

Lu, Y., Wen, Z., Shi, D., Chen, M., Zhang, Y., Bonnet, S., Li, Y., Tian, J., and Kao, S. J.: Effect of light on N_2 fixation and net nitrogen release of *Trichodesmium* in a field study, Biogeosciences, 15, 1–12, doi: 10.5194/bg-15-1-2018, 2018.

Mackinder, L., Wheeler, G., Schroeder, D., von Dassow, P., Riebesell, U., and Brownlee, C.: Expression of biomineralization-related ion transport genes in *Emiliania huxleyi*, Env. Microbiol., 13, 3250–3565, doi:10.1111/j.1462-2920.2011.02561.x, 2011.

Masuko, T., Minami, A., Iwasaki, N., Majima, T., Nishimura, S. I., and Lee, Y. C.: Carbohydrate analysis by a phenol-sulfuric acid method in microplate format, Anal. Biochem., 339, 69–72, doi: 10.1016/j.ab.2004.12.001, 2005.

Matthiessen, B., Eggers, S. L., and Krug, S. A.: High nitrate to phosphorus regime attenuates negative effects of rising pCO_2 on total population carbon accumulation, Biogeosciences, 9, 1195–1203, doi: 10.5194/bg-9-1195-2012,

776   2012.

777 McKew, B. A., Metodieva, G., Raines, C. A., Metodiev, M. V., and Geider, R. J.:

778   Acclimation of *Emiliania huxleyi* (1516) to nutrient limitation involves precise

779   modification of the proteome to scavenge alternative sources of N and P,

780   Environ. Microbiol., 17, 4050–4062, doi: 10.1111/1462-2920.12957, 2015.

781 Meyer, J., and Riebesell, U.: Reviews and syntheses: responses of coccolithophores to

782   ocean acidification: a meta-analysis, Biogeosciences, 12, 1671–1682, doi:

783   10.5194/bg-12-1671-2015, 2015.

784 Moreno, A. R., and Martiny, A. C.: Ecological stoichiometry of ocean plankton, Ann.

785   Rev. Mar. Sci., 10, 43–69, doi: 10.1146/annurev-marine-121916-063126, 2018.

786 Müller, M. N., Antia, A. N., and LaRoche, J.: Influence of cell cycle phase on

787   calcification in the coccolithophore *Emiliania huxleyi*, Limnol. Oceanogr., 53,

788   506–512, doi: 10.4319/lo.2008.53.2.0506, 2008.

789 Ni, G., Zimbalatti, G., Murphy, C. D., Barnett, A. B., Arsenault, C. M., Li, G.,

790   Cockshutt, A. M., and Campbell, D. A.: Arctic *Micromonas* uses protein pools

791   and non-photochemical quenching to cope with temperature restrictions on

792   Photosystem II protein turnover, Photosynth. Res., 131, 203–220, doi:

793   10.1007/s11120-016-0310-6, 2016.

794 Pakulski, J. D., and Benner, R.: An improved method for the hydrolysis and MBTH

795   analysis of dissolved and particulate carbohydrates in seawater, Mar. Chem., 40,

796   143–160, doi: 10.1016/0304-4203(92)90020-B, 1992.

797 Perrin, L., Probert, I., Langer, G., and Aloisi, G.: Growth of the coccolithophore

798   *Emiliania huxleyi* in light- and nutrient-limited batch reactors: relevance for the

799   BIOSOPE deep ecological niche of coccolithophores, Biogeosciences, 13, 5983–

800   6001, doi: 10.5194/bg-13-5983-2016, 2016.

Pierrot, D., Lewis, E., and Wallace, D. W. R.: MS Excel program developed for CO_2 system calculations, ORNL/CDIAC-105, Carbon Dioxide Information Analysis Centre, Oak Ridge National Laboratory, U.S., Department of Energy, doi: 10.3334/CDIAC/otg.CO2SYS_XLS_CDIAC105a, 2006.

R version 3.5.0.: The R foundation for statistical computing platform, x86_64-w64-mingw32/x64. Available from: https://cran.r-project.org/bin/windows/ base/old/3.5.0, 2018.

Reith, M. E., and Cattolico, R. A.: Chloroplast protein synthesis in the chromophytic alga *Olisthodiscus luteus*, Plant Physiol., 79, 231–236, doi: 10.1104/pp.79.1.231, 1985.

Riebesell, U., Bach, L. T., Bellerby, R. G. J., Rafael Bermúdez Monsalve, J., Boxhammer, T., Czerny, J., Larsen, A., Ludwig, A., and Schulz, K. G.: Competitive fitness of a predominant pelagic calcifier impaired by ocean acidification, Nat. Geosci., 10, 19–24, dio: 10.1038/NGEO2854, 2017.

Riegman, R., Stolte, W., Noordeloos, A. A. M., and Slezak, D.: Nutrient uptake and alkaline phosphatase (EC 3:1:3:1) activity of *Emiliania huxleyi* (Prymnesiophyceae) during growth under N and P limitation in continuous cultures, J. Phycol., 36, 87–96, 2000.

Rokitta, S. D., von Dassow, P., Rost, B., and John, U.: P- and N-depletion trigger similar cellular responses to promote senescence in eukaryotic phytoplankton, Front. Mar. Sci., 3, 109, doi: 10.3389/fmars.2016.00109, 2016

Rokitta, S. D., and Rost, B: Effects of CO_2 and their modulation by light in the life-cycle stages of the coccolithophore *Emiliania huxleyi*, Limnol. Oceanog., 57, 607–618, doi: 10.4319/lo.2012.57.2.0607, 2012.

Rokitta, S. D., de Nooijer, L. J., Trimborn, S., de Vargas, C., Rost, B., and John, U.:

826   Transcriptome analyses reveal differential gene expression patterns between the

827   life-cycle stages of *Emiliania huxleyi* (haptophyta) and reflect specialization to

828   different ecological niches, J. Phycol., 47, 829–838, doi:

829   10.1016/S0924-9338(02)00624-7, 2011.

830   Rost, B., and Riebesell, U.: Coccolithophores and the biological pump: responses to

831   environmental changes, in: Coccolithophores : from molecular biology to global

832   impact, edited by: Thierstein, H. R. and Young, J. R., Springer, Berlin, 99–125,

833   2004.

834   Rouco, M., Branson, O., Lebrato, M., and Iglesias-Rodríguez, M.: The effect of

835   nitrate and phosphate availability on *Emiliania huxleyi* (NZEH) physiology

836   under different CO_2 scenarios, Front. Microbiol., 4, 1–11, doi:

837   10.3389/fmicb.2013.00155, 2013.

838   Roy, R. N., Roy, L. N., Vogel, K. M., Porter-Moore, C., Pearson, T., Good, C. E.,

839   Millero, F. J., and Campbell, D. C.: Thermodynamics of the dissociation of boric

840   acid in seawater at S 5 35 from 0 degrees C to 55 degrees C, Mar. Chem., 44,

841   243–248, doi: 10.1016/0304-4203(93)90206-4, 1993.

842   Shemi, A., Schatz, D., Fredricks, H. F., Van Mooy, B. A. S., Porat, Z., and Vardi, A.:

843   Phosphorus starvation induces membrane remodeling and recycling in *Emiliania*

844   *huxleyi*, New Phytol., 211, 886–898, doi: 10.1111/nph.13940, 2016.

845   Solórzano, L., and Sharp, J. H.: Determination of total dissolved phosphorus and

846   particulate phosphorus in nature waters, Limnol. Oceanogr., 25, 754–758, doi:

847   10.4319/lo.1980.25.4.0754, 1980.

848   Steinacher, M., Joos, F., Frölicher, T. L., Bopp, L., Cadule, P., Cocco, V., Doney, S.

849   C., Gehlen, M., Lindsay, K., Moore, J. K., Schneider, B., and Segschneider, J.:

850   Projected 21st century decrease in marine productivity: a multi-model analysis,

851   Biogeosciences, 7, 979–1005, doi: 10.5194/bg-7-979-2010, 2010.

852   Sterner, R. W., and Elser, J. J.: Ecological Stoichiometry: The Biology of Elements

853   from Molecules to the Biosphere, Princeton University Press, Princeton, 2002.

854   Terrats, L., Claustre, H., Cornec, M., Mangin, A., and Neukermans, G.: Detection of

855   coccolithophore blooms with BioGeoChemical-Argo floats, Geophys. Res. Lett.,

856   47, e2020GL090559, doi: 10.1029/2020GL090559, 2020.

857   Townsend, D. W., Keller, M. D., Holligan, P. M., Ackleson, S. G., and Balch, W. M.:

858   Blooms of the coccolithophore *Emiliania huxleyi* with respect to hydrography in

859   the Gulf of Maine, Cont. Shelf Res., 14, 979–1000, doi:

860   10.1016/0278-4343(94)90060-4, 1994.

861   Tyrrell, T., and Merico, A.: *Emiliania huxleyi*: bloom observations and the conditions

862   that induce them, in: Coccolithophores : from molecular biology to global impact,

863   edited by: Thierstein, H. R. and Young, J. R., Springer, Berlin, 75–97, 2004.

864   Wang, C., Wang, J., Li, L., Wang, Y., and Lin, S.: P-limitation promotes carbon

865   accumulation and sinking of *Emiliania huxleyi* through transcriptomic

866   reprogramming, Front. Mar. Sci., 9, 860222, doi: 10.3389/fmars.2022.860222,

867   2022.

868   Wang, G., Xie, S. P., Huang, R. X., and Chen. C.: Robust warming pattern of global

869   subtropical oceans and its mechanism, J. Climate, 28, 8574–8584, doi:

870   10.1175/jcli-d-14-00809.1, 2015.

871   Wilson, D. N., and Doudna Cate J. H.: The structure and function of the eukaryotic

872   ribosome, CSH Perspect. Biol., 4, a011536, doi: 10.1101/cshperspect.a011536,

873   2012.

874   Zhang, Y., Collins, S., and Gao, K.: Reduced growth with increased quotas of

875   particulate organic and inorganic carbon in the coccolithophore *Emiliania*

huxleyi under future ocean climate change conditions, Biogeosciences, 17, 6357–6375, doi: 10.5194/bg-17-6357-2020, 2020.

Zhang, Y., Li, Z. K., Schulz, K. G., Hu, Y., Irwin, A. J., and Finkel, Z. V.: Growth-dependent changes in elemental stoichiometry and macromolecular allocation in the coccolithophore *Emiliania huxleyi* under different environmental conditions, Limnol. Oceanogr., 66, 2999–3009, doi: 10.1002/lno.11854, 2021.

 Figure Legends

902 **Figure 1.** Growth rate (**a**), cellular contents of particulate organic carbon (POC, **b**),

903 nitrogen (PON, **c**) and phosphorus (POP, **d**), and particulate inorganic carbon (PIC, **e**)

904 of *Emiliania huxleyi* RCC1266 in the treatments of high phosphorus availability and

905 low CO_2 level (HP+LC), high phosphorus availability and high CO_2 level (HP+HC),

906 low phosphorus availability and low CO_2 level (LP+LC), and low phosphorus

907 availability and high CO_2 level (LP+HC) under low light (empty, 40 μmol photons

908 m^{-2} s^{-1}) and high light (fill, 300 μmol photons m^{-2} s^{-1}) intensities. Different letters

909 represent significant differences in each parameters between treatments ($p < 0.05$).

910 The data represents the means and standard deviation of four independent cultures.

911

912 **Figure 2.** Cellular contents of carbohydrate (**a**) and protein (**b**), and the percentages of

913 POC allocated to carbohydrate (**c**) and protein (**d**), and the percentage of PON

914 allocated to protein (**e**) of *E. huxleyi* RCC1266 in the treatments of high phosphorus

915 availability and low CO_2 level (HP+LC), high phosphorus availability and high CO_2

916 level (HP+HC), low phosphorus availability and low CO_2 level (LP+LC), and low

917 phosphorus availability and high CO_2 level (LP+HC) under low light (empty) and

918 high light (fill) intensities. Different letters represent significant differences in each

919 parameters between treatments ($p < 0.05$). The data represents the means and standard

920 deviation of four independent cultures.

921

922 **Figure 3.** Cellular POC : POP ratio (**a**), PON : POP ratio (**b**), and protein content (**c**)

923 of *E. huxleyi* RCC1266 as a function of growth rate, and cellular POC content as a

924 function of carbohydrate (**d**) in the treatments of high phosphorus availability and low

925 CO_2 level (HP+LC, □), high phosphorus availability and high CO_2 level (HP+HC,

926   ○), low phosphorus availability and low CO_2 level (LP+LC, △), and low phosphorus

927   availability and high CO_2 level (LP+HC, ◇) under low light (LL, empty) and high

928   light (HL, fill) intensities. Each point indicates an individual replicate under each

929   treatment.

930

931

932

933

934

935

936

937

938

939

940

941

942

943

944

945

946

947

948

949

950

Table 1. Carbonate chemistry parameters and dissolved inorganic phosphorus (DIP) concentration at the end of the incubation. The values are means ± standard deviation (sd) of four replicates. Respectively, LL and HL represent 40 and 300 μmol photons m^{-2} s^{-1} of photosynthetically active radiation (PAR), and HP and LP represent 4 and 0.43 μmol L^{-1} PO$_4^{3-}$ at the beginning of the incubations.

			pCO$_2$ (μatm)	pH (total scale)	TA (μmol L^{-1})	DIC (μmol L^{-1})	HCO$_3^-$ (μmol L^{-1})	CO$_3^{2-}$ (μmol L^{-1})	DIP (μmol L^{-1})
LL	HP	LC	403±4	8.06±0.01	2346±23	2074±21	1861±18	200±2	3.20±0.03
		HC	881±20	7.77±0.01	2351±33	2216±32	2074±30	114±2	3.12±0.08
	LP	LC	329±4	8.13±0.01	2332±24	2024±22	1787±19	225±3	<0.04
		HC	730±8	7.84±0.01	2349±24	2189±23	2033±22	132±2	<0.04
HL	HP	LC	357±9	8.09±0.01	2235±41	1959±35	1749±30	199±6	2.86±0.06
		HC	791±7	7.80±0.01	2296±20	2151±20	2007±18	118±1	2.70±0.06
	LP	LC	303±4	8.16±0.01	2354±13	2024±11	1773±9	241±3	<0.04
		HC	735±19	7.83±0.01	2319±69	2162±65	2011±60	128±5	<0.04

Table 2. Growth rate (d^{-1}), cellular contents of POC, PON, POP, PIC, carbohydrate (CHO) and protein (Pro) (pg cell^{-1}), and the ratios of POC : PON, POC : POP, PON : POP and PIC : POC, and the percentages of POC allocated to carbohydrate (CHO–C : POC) and protein (Pro–C : POC), and the percentage of PON allocated to protein (Pro–N : PON) (%). LC and HC represent low CO_2 (426 µatm) and high CO_2 (946 µatm) levels, respectively. Please see table 1 for more detailed information.

| | Low light intensity | | | | High light intensity | | | |
| | HP | | LP | | HP | | LP | |
	LC	HC	LC	HC	LC	HC	LC	HC
Growth rate	0.91±0.03	0.88±0.01	0.83±0.02	0.70±0.03	1.35±0.03	1.33±0.02	1.34±0.02	1.12±0.02
POC	8.34±0.57	8.73±0.32	8.20±0.36	8.04±0.24	10.53±0.70	11.04±0.42	11.73±0.19	12.70±0.50
PON	1.49±0.16	1.58±0.12	1.23±0.06	1.20±0.10	1.65±0.05	1.89±0.07	1.51±0.07	1.56±0.06
POP	0.16±0.01	0.15±0.01	0.08±0.01	0.07±0.01	0.22±0.01	0.21±0.01	0.12±0.01	0.10±0.01
PIC	2.12±0.22	1.45±0.17	2.44±0.11	2.06±0.37	3.74±0.22	2.41±0.41	4.83±0.34	3.79±0.49
POC:PON	6.57±0.43	6.46±0.52	7.78±0.46	7.87±0.54	7.45±0.28	6.83±0.32	9.09±0.44	9.50±0.11
POC:POP	133.3±7.8	153.8±13.9	282.4±31.2	313.0±40.5	124.2±3.5	137.8±8.5	259.7±23.2	316.9±30.4
PON:POP	20.40±2.53	23.98±3.37	36.30±3.54	40.10±7.42	16.68±0.47	20.21±1.47	28.63±2.80	33.33±2.85
PIC:POC	0.26±0.04	0.17±0.02	0.30±0.02	0.26±0.04	0.36±0.02	0.22±0.04	0.41±0.03	0.30±0.04
CHO	1.45±0.15	1.81±0.16	1.79±0.16	1.94±0.16	3.58±0.41	4.30±0.17	4.96±0.24	5.85±0.49
Protein	5.23±0.55	5.37±0.39	3.73±0.27	3.80±0.15	6.45±0.36	6.97±0.22	6.25±0.29	6.28±0.30
CHO–C:POC	6.95±0.41	8.31±0.85	8.71±0.70	9.64±0.58	13.62±1.43	15.60±0.98	16.92±1.04	18.39±0.96
Pro–C:POC	33.26±3.24	32.58±1.98	24.15±2.52	25.07±1.69	32.49±1.69	33.51±1.41	28.23±1.35	26.21±1.27
Pro–N:PON	56.84±8.96	54.55±6.51	48.41±2.46	51.07±5.40	62.62±2.88	59.12±1.21	66.35±4.06	64.44±2.73

989   Figure 1

992
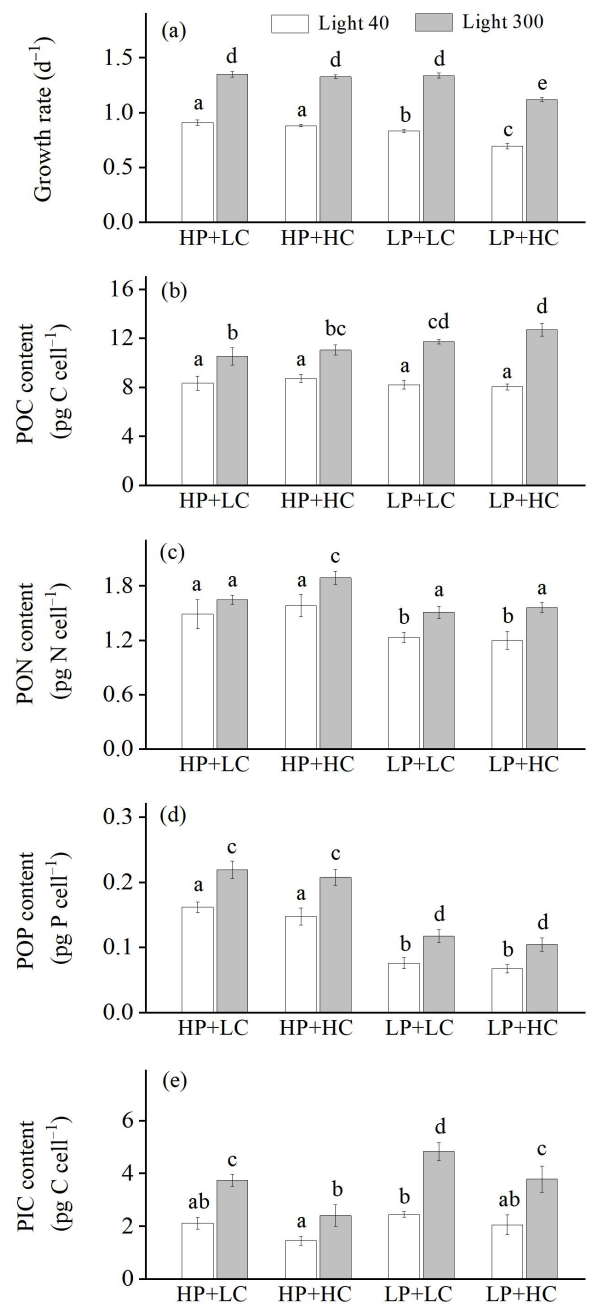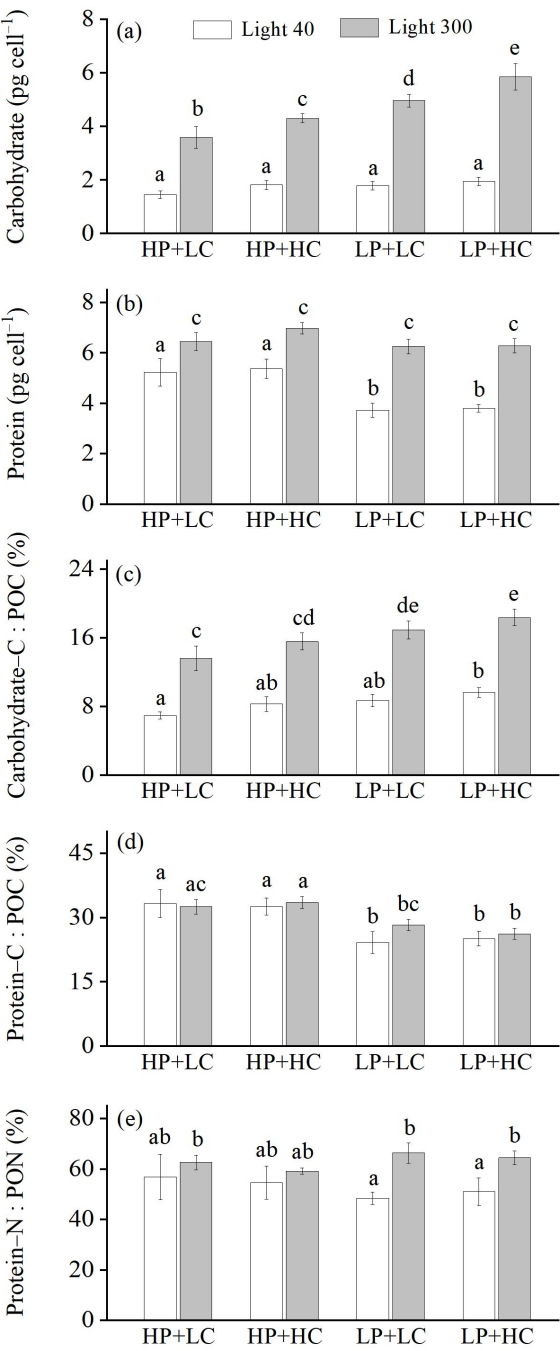
993

994

995   Figure 2

996

997

998

999

1000

1001   Figure 3

1002

1003